FACULTY OF CHEMISTRY AND CHEMICAL ENGINEERING
"BABEŞ-BOLYAI" UNIVERSITY, CLUJ-NAPOCA

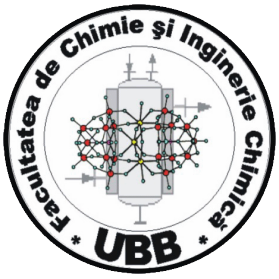

PhD Thesis Abstract

***SILAI** (căs. **KILLYÉNI**) Catalina Anikó*

Modified electrodes with molecular recognition properties

Jury:

President:

Prof. Liana Maria MUREŞAN, Babeș-Bolyai University, Cluj-Napoca

Scientific advisor:

Prof. Ionel Cătălin POPESCU

Members:

Prof. Camellia BALA, University of București

Prof. Lo GORTON, Lund University, Sweden

Conf. Graziella TURDEAN, Babeș-Bolyai University, Cluj-Napoca

Defense: 26th of August 2013

TABLE OF CONTENTS

Keywords: *Pyranose dehydrogenase, osmium redox polymer, mediated electron transfer, enzyme deglycosylation, substrate selectivity, calix[8]arene, adsorption kinetics, SAM reorganization, Electrochemical impedance spectroscopy, quartz crystal microbalance*

1. INTRODUCTION

Over the past century many studies have been published searching an efficient and simple route to functionalize metallic surface with various molecules. The integration of enzymes aiming at increase the bio/electrodes selectivity is well established, but there are still many challenges in this field (Frew *et al.* 1987).

Pyranose dehydrogenase (PDH; EC 1.1.99.29) is a monomeric sugar oxidoreductase and is produced in a narrow group of fungi, classified, based on the ecophysiological characteristics, as litter-decomposing fungi. PDH carries one covalently bound flavin adenine dinucleotide (FAD)(Sygmund *et al.* 2008) as the prosthetic group (Figure 1).

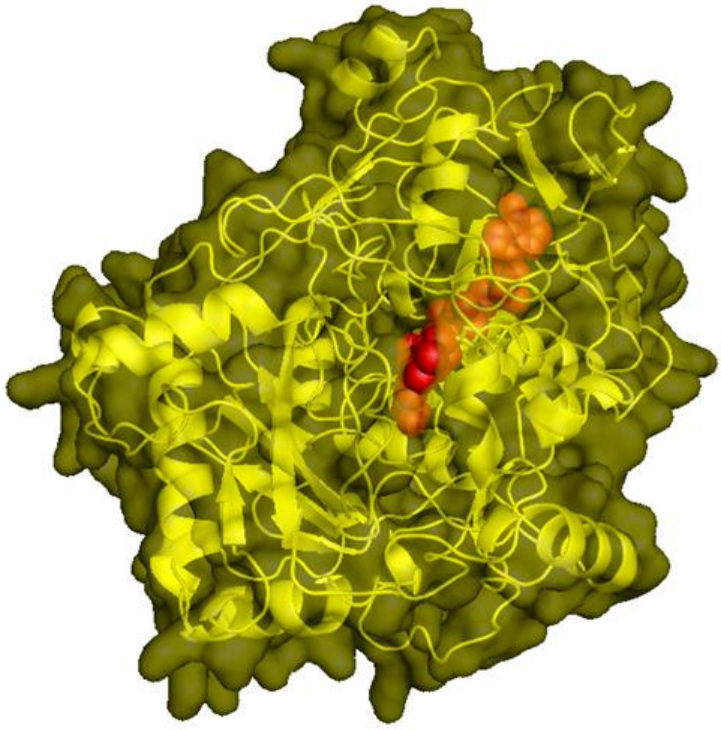

Figure 1. PDH isolated from *Agaricus meleagris (Am)* enzyme with covalently bound FAD domain in red.

Depending on the enzyme source and the substrate, PDH can catalyze the mono- and dioxidation of a variety of sugars at C-2, C-3 and C-2,3C-3,4 positions to their corresponding aldonolactones, or (di)dehydrosugars (aldos(di)uloses) (Volc *et al.* 1998; Volc *et al.* 2002; Peterbauer *et al.* 2010) with the equal catalytic efficiency which makes the enzyme attractive for application in analytical chemistry, industrial production of rare sugars, and construction of enzymatic biofuel cells (EBFC).

Glycosylation is one of the most common modifications of the proteins. More than 50 % of the studied proteins are glycosylated. By removing the glycan shell from the enzyme molecule, a decrease of the distance between the enzyme redox center and the electrode surface can be observed (Lindgren *et al.* 1999; Presnova *et al.* 2000; Ferapontova *et al.* 2001; Prévoteau *et al.* 2010) and, according to the Marcus equation (Marcus 1964), direct electron transfer should be facilitated.

The molecular weight (MW) of *Am*PDH expressed in *P. pastoris* was determined by SDS-PAGE to be ~93 kDa, corresponding to an excessive glycosylation of ~30%, whereas the native *Am*PDH has a MW of ~66.5 kDa with 7% glycosylation (Sygmund *et al.* 2008).

The deglycosylation of enzymes can offer new possibilities to increase the biocatalytic efficiency of bioelectrodes, as it has been observed previously for both direct (Lindgren *et al.* 1999; Presnova *et al.* 2000; Ferapontova *et al.* 2001; Ferapontova *et al.* 2005; Ortiz *et al.* 2012) and mediated electron transfer (Fraser *et al.* 1992; Courjean *et al.* 2010; Prévoteau *et al.* 2010).

Among the different approaches for the preparation of molecular designed electrochemical interfaces, the self-assembled monolayers have been proved to have a remarkable efficiency and versatility (Buck 2009). Consequently, a large number of fundamental and applied studies exploiting self-assembled structures have been published.

Calixarenes are a class of cyclo-oligomers. They can exist in a cuplike shape with an upper and a lower rim and a central annulus. Due to their structure, the selectivity of calixarenes can be controlled by functionally modifying either the upper or the lower rim. Calixarenes exhibit a pronounced conformational flexibility, easy to be controlled by the proper design of the skeleton size and/or by the substituent's nature (Lucke *et al.* 2000; Gutsche 2008), which will decisively influence the compromise between the versatility and the selectivity of the recognition process.

The calixarene derivatives adsorbed on metallic surfaces, are able to recognize different chemical species like: cations of alkaline, earth alkaline (Chung *et al.* 2001; Sakly *et al.* 2007; Chen *et al.* 2008; Chen *et al.* 2010b), transition metals (Wang *et al.* 2001; Zhang *et al.* 2003; Becker *et al.* 2008), anions (Zhang *et al.* 2006) and biomolecules as well (Zhang *et al.* 2004; Huang *et al.* 2005; Hassen *et al.* 2007; Patel *et al.* 2009; Bian *et al.* 2010; Chen *et al.* 2010a; Šnejdárková *et al.* 2010; Chen *et al.* 2013).

In this thesis two approaches for electrode modification are described:

(i) The first one is based on the immobilization of deglycosylated *Am*PDH (dgPDH) for improving the biocatalytic properties of the dgPDH based bioelectrode;

(ii) The second one uses the absorption of thioacetylated calix[8]arene on gold surface in order to obtain a smart interface, able to recognize various chemical species.

The thesis is structured into two main parts: a bibliographical overview and the original contributions. In the bibliographic part the following topics are highlighted: biosensors, electron transfer between the enzymes redox center and the electrode, pyranose dehydrogenases and its molecular properties, self-assembled monolayers on gold and calixarenes, and a short description of the methods used to perform the experimental investigations. The original contribution is structured into two separate parts: the effect of deglycosylation of PDH on its electrocatalytic activity is discussed in the first part, while, in the second part, a kinetic study of the adsorption of thioacetylated calix[8]arene on gold is presented.

2. THE MAIN OBJECTIVES OF THE THESIS

There have been many researches in the past three decades which tries to dispel the fog from the domain of modified electrodes. The present thesis has the will to:

(i) Characterize and develop a new bioelectrode with improved biocatalytic properties, based on enzyme deglycosylation;

(ii) Investigate the reorganization process observed in the case of a SAM, built up by the adsorption of S-Calix on polycrystalline gold surface.

3. EFFECT OF DEGLYCOSYLATION ON THE MEDIATED ELECTROCATALYTIC ACTIVITY OF RECOMBINANTLY EXPRESSED *Am*PDH WIRED BY OS-RP

The effect of deglycosylation on the bioelectrocatalytic activity of PDH was investigated by carrying out the immobilization of gPDH or dgPDH on the surface of graphite electrode (Killyeni *et al.* 2012; Yakovleva *et al.* 2012; Killyéni *et al.* 2013).

The enzyme immobilization was done by simple adsorption of the dissolved enzymes from a mixture containing the osmium redox polymer and a cross-linking agent (PEGDGE).

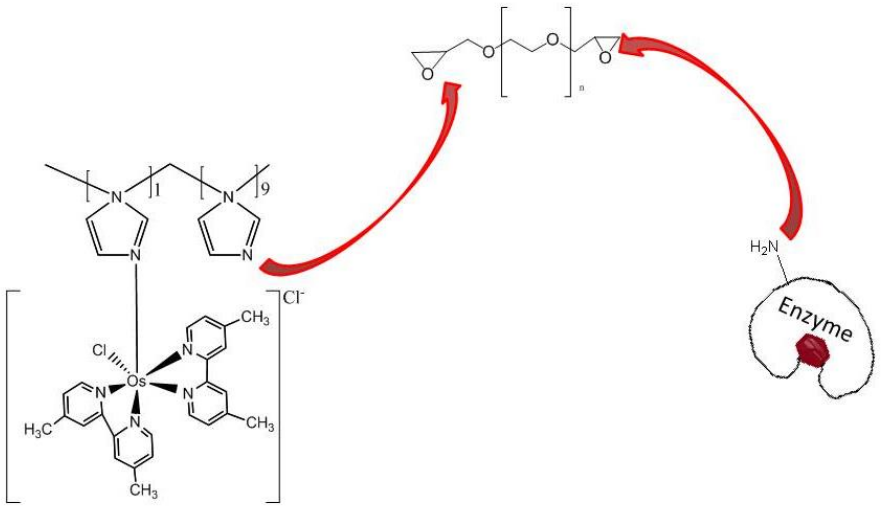

Figure 2. Schematic presentation of cross-linking reaction of Os-RPII and enzyme using PEGDGE as a cross-linking agent.

The cross-linking reaction is presented in Figure 2, the water soluble diepoxide is able to crosslinks primary, secondary, and tertiary amines, as well as heterocyclic nitrogen**.** In order to perform a reliable comparison, equal amounts (in terms of activity) of gPDH and dgPDH were deposited on the electrode surface.

3.1. Optimization of the bioelectrodes

The response of a bioelectrode is highly influenced by some key working parameters such as applied potential, working pH, flow rate and also the structure of the bioelectrode is playing an important role. In order to have an efficient system the optimization of this key parameter is required.

i. Osmium Redox Polymers

For wiring *Am*PDHs on graphite electrodes two water soluble osmium redox polymers (Os-RP) were tested with different formal potentials.

The maximum amperometric response recorded at G/gPDH-(Os-RPII) electrode is approximately 3.5 times higher than that measured for G/gPDH-(Os-RPI) electrode. For an efficient electron transfer Os-RPII, having a E°′ value of +32 mV *vs.* Ag|AgCl, 0.1M KCl, was chosen to connect electrically the enzyme redox center to the electrode.

ii. Flow rate

*Am*PDH can oxidize D-glucose transiently to 2-dehydro-D-glucose or 3-dehydro-D-glucose and, further to 2,3-didehydro-D-glucose (Peterbauer *et al.* 2010). Therefore, taking into account this complex behavior of PDH it was interesting to evaluate the influence of the flow rate (studied domain 0.1 -1.8 mL/min) on the current response of the modified bioelectrodes. As expected for transient measurements, the increase in the flow carrier rate leads to a clear decrease in the current response.

All measurements were performed at a flow rate of 0.45 mL/min. For this flow rate value, both types of biosensors showed a minor decrease in the current response (less than 10%).

iii. Applied potential

For an applied potential higher than +200 mV *vs.* Ag|AgCl, 0.1 M KCl, for both investigated bioelectrodes, a steady-state response is reached (Figure 3). Consequently, aiming to achieve the highest sensitivity at the lowest value of the applied potential, an applied potential of +200 mV *vs.* Ag|AgCl, 0.1M KCl was chosen for all further measurements.

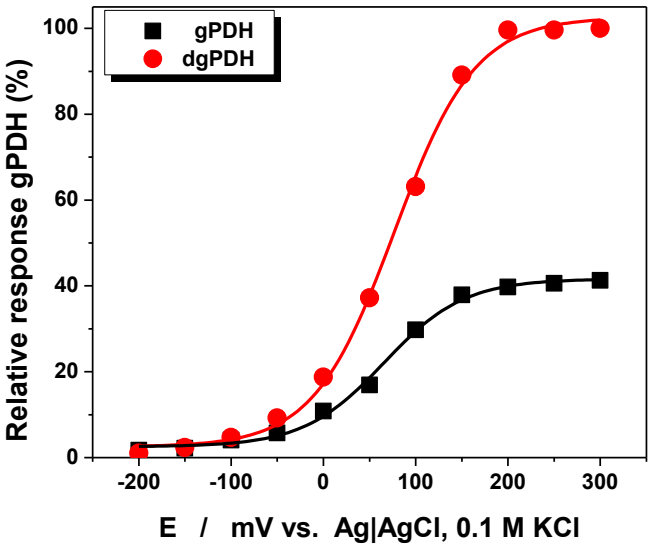

Figure 3. Dependence of the amperometric response on the applied potential observed at G/gPDH-(Os-RPII) and G/dgPDH-(Os-RPII) modified electrodes.
Experimental conditions: enzyme loading, 17.6 U/cm; 10 mg/mL Os-RPII; supporting electrolyte, 50 mM PB containing 137 mM NaCl (pH 7.4); flow rate, 0.45 mL/min; injected sample, 50 µL of 5 mM glucose.

iv. Enzyme loading

In order to optimize the amount of the immobilized enzyme, bioelectrodes incorporating *Am*PDH-(Os-RPII) were realized with different enzyme loading. For an enzyme loading of 23.6 Ucm^{-2} the highest current was registered for both modified electrodes. For higher enzyme loading the current response was almost the same, while for lower enzyme loading it was significantly lower.
Consequently, irrespective the type of *Am*PDH immobilized on the graphite electrode surface, an enzyme loading of 23.6 Ucm^{-2} was taken as the optimum value

v. Working pH

A small difference was noticed between the values corresponding to the optimum pH for gPDH (pH 9) and dgPDH (pH 9.5). However, all further experiments were done at a pH value corresponding to the physiological conditions (pH 7.4).

3.2. Kinetic parameters

In order to evaluate the kinetic parameters of *Am*PDH modified electrode both gPDH and dgPDH based bioelectrode were investigated in FIA system and the obtained calibration curves for glucose are showed in Figure 4 A. The kinetic parameters corresponding to the investigated bioelectrodes were estimated by fitting the calibration curves for glucose to the Michaelis-Menten equation (Table 1).

Table 1. Comparison of the kinetic parameters of gPDH and dgPDH based bioelectrodes using glucose as substrate (*for experimental conditions see; 10 mg/mL Os-RPII)*

Bioelectrode	**j_{max} (μAcm^{-2})**	**K_M^{app} (mM)**	**DL* (mM)**	**Linear range (mM)**	**No. of tested electrodes**
G/gPDH-(Os-RPII)	80.9 ± 1.9	7.5 ± 0.3	0.01	0.1-1	5
G/dgPDH-(Os-RPII)	146.6 ± 2.6	2.4 ± 0.1	0.003	0.1-1	5

*estimated for signal/noise ratio of 3.

The biosensor based on dgPDH showed a significantly higher catalytic current density than that observed for gPDH. This finding proves once again the higher bioelectrocatalytic activity of the deglycosylated *Am*PDH.

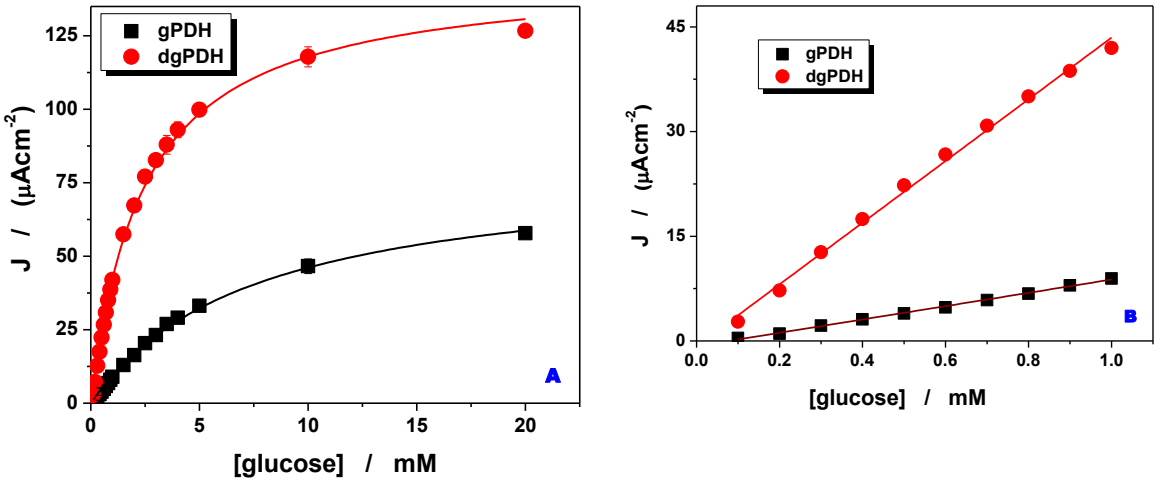

Figure 4 (A) Calibration curves and (B) the linear domain of G/gPDH-(Os-RPII) and of G/gPDH-(Os-RPII) bioelectrodes using glucose as substrate.
Experimental conditions: applied potential, +200 mV vs. Ag|AgCl, 0.1M KCl; enzyme loading, 17.6 Ucm^{-2}; 10 mg/mL Os-RPII; supporting electrolyte, 50 mM PB containing 137 mM NaCl (pH 7.4); flow rate, 0.45 mL/min.

At the same time, *Am*PDH deglycosylation resulted in a lower value of the apparent Michaelis constant, compared with that estimated for glycosylated enzyme. This behavior suggests either:

(i) higher enzyme-substrate affinity for dgPDH, or

(ii) higher permeability to glucose of the deglycosylated enzyme matrix associated with a higher accessibility of the Os-RP for the deglycosylated enzyme.

For both modified bioelectrodes the linear range was practical the same, from 0.1 up to 1 mM glucose (Figure 4 B), while the detection limits were significantly different: 0.01 and 0.003 mM for glycosylated and deglycosylated *Am*PDH, respectively.

The slope of the linear domain for G/dgPDH-(Os-RPII) bioelectrode [(43.6 ± 1.1) μA/(mM/cm^2)] was almost 4.5 times higher than that for G/gPDH-(Os-RPII) bioelectrode [(9.74 ± 0.16) μA/(mM/cm^2)].

At the same enzyme loading (expressed in Ucm^{-2}), the G/dgPDH-(Os-RPII) bioelectrode exhibits a higher amperometric response compared with the G/gPDH-(Os-RPII) bioelectrode probably due to:

(i) a faster electron transfer between the Os-RP and the covalently bound FAD cofactor of dgPDH;

(ii) an increase in the substrate accessibility at the dgPDH active center, induced by the higher permeability of the Os-RP – dgPDH network (Prévoteau *et al.* 2010).

3.3. Short term stability

The operational stability of a bioelectrode is one of the key parameters and further it was evaluated by carrying out a test of short term stability under a constant flow of 5 mM glucose (Figure 5).

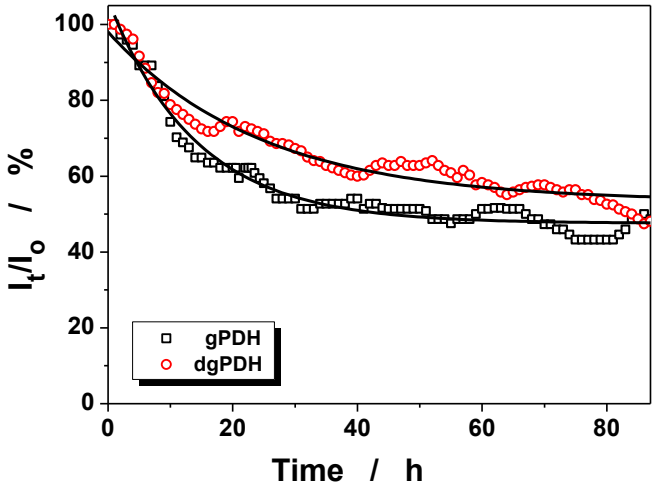

Figure 5. **S**tability of G/gPDH-(Os-RPII) and G/dgPDH-(Os-RPII) bioelectrodes under continuous flow of 5 mM glucose.
Experimental conditions: applied potential, +200 mV vs. Ag|AgCl, 0.1M KCl; enzyme loading, 23.6 Ucm^{-2}; 5 mg/mL Os-RPII; supporting electrolyte, 50 mM PB (pH 7.4); flow rate, 0.45 mL/min. The solid lines stand for the fitting of experimental data by the equation describing an exponential decay of the bioelectrode response.

For both modified electrodes, a pronounced decrease in the current response during the first 20 hours was observed. Thus, for G/dgPDH-(Os-RPII) the decrease was ~26 %, while for G/gPDH-(Os-RPII) the decrease in the response was more accentuated (~38 %).

3.4. Substrate selectivity

*Am*PDH showed a notable bioelectrocatalytic activity toward various sugars such as: 2-deoxy-*D*-galactose, cellobiose, fucose, sucrose, trehalose, galactose, xylose (Tasca *et al.* 2007). In order to establish if the enzyme deglycosylation induces changes in the selectivity order of *Am*PDH, the kinetic parameters corresponding to the G/gPDH-(Os-RPII) and G/dgPDH-(Os-RPII) bioelectrodes were estimated by fitting the calibration curves recorded for glucose, galactose, lactose, maltose, mannose, cellobiose, 2-deoxy-*D*-glucose, fucose, sucrose and xylose to the Michaelis-Menten equation. The sensitivity of G/gPDH-(Os-RPII) and G/dgPDH-(Os-RPII) for all investigated sugars was estimated as the I_{max}/K_M^{app} ratios (Figure 6).

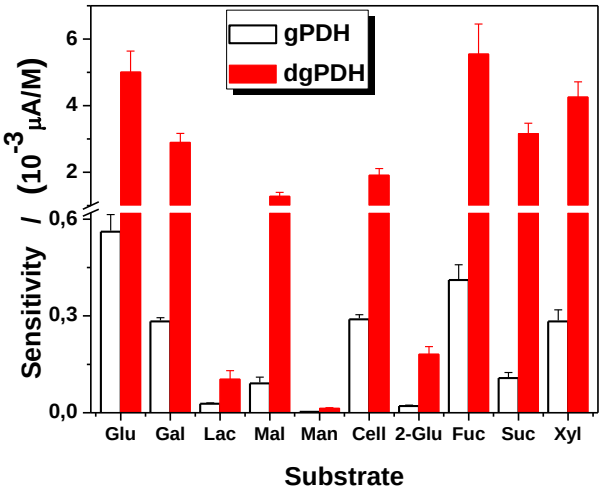

Figure 6. Sensitivities of the G/gPDH-(Os-RPII) and G/dgPDH-(Os-RPII) modified electrodes towards different substrates: *Glu*, glucose; *Gal*, galactose; *Lac*, lactose; *Mal*, maltose; *Man*, mannose; *Cell*, cellobiose; *2-Glu*, 2-deoxy-*D*-glucose; *Fuc*, fucose; *Suc*, sucrose; *Xyl*, xylose.
Experimental conditions: applied potential, +200 mV vs. Ag|AgCl, 0.1M KCl; enzyme loading, 23.6 Ucm^{-2}; 5 mg/ml Os-RPII; supporting electrolyte, 50 mM PB containing 137 mM NaCl (pH 7.4); flow rate, 0.45 mL/min

As can be seen from Figure 6 *Am*PDH deglycosylation induces significant changes in the order of substrate selectivity:

- **gPDH:** Glucose > Fucose > Galactose > Cellobiose > Xylose > Sucrose > Maltose > Lactose > 2-Deoxy-*D*-glucose > Mannose
- **dgPDH:** Fucose > Glucose > Xylose > Sucrose > Galactose > Cellobiose > Maltose > 2-Deoxy-*D*-glucose > Lactose > Mannose

3.5. Further decomposition of deglycosylated AmPDH, storage conditions influence

It was accidently discovered that when stored under certain conditions, dgPDH loses almost 20 kDa from its C-terminus (Yakovleva *et al.* 2013). The loss of a peptide fragment from dgPDH C-terminus part results in the formation of a stable deglycosylated PDH (sdgPDH).

In order to follow the decomposition process a portion of freshly purified and enzymatically deglycosylated PDH was stored at 4 °C instead of -30 °C, temperature at which the enzyme showed to be stable (Sygmund *et al.* 2012).

The fragmentation process was followed by gel electrophoresis (SDS-PAGE) and measurements of the enzyme activity by using ferrocenium ion (Fc^+) as electron acceptor. All three *Am*PDH forms (gPDH, dgPDH and sdgPDH) were electrically "wired" to an Os based redox polymer (Os-RPII) on the surface of graphite electrodes. The current outputs accompanying the biocatalytic oxidation of glucose at gPDH, dgPDH or sdgPDH based bioelectrodes were compared using FI and CV *(results in the thesis*).

3.5.1. Gel electrophoresis study of dgPDH decomposition

All three forms of PDH (gPDH, dgPDH and sdgPDH) were investigated using SDS-PAGE stained with silver (Bartsch *et al.* 2012). The molecular weight of gPDH recombinantly expressed in *P. pastoris* was determined to be roughly ~95 kDa (Figure 7 A, B), similar to previous reports (Sygmund *et al.* 2012). gPDH appears in a broad band due to the possible structural variations in the glycan moieties (Mechref *et al.* 2002). A major band at ~65 kDa corresponds to dgPDH (release of ~30-35 kDa of glycan moiety). A minor band at ~46 kDa is presumably the stable deglycosylated PDH (sdgPDH) which is formed when the enzyme is stored at +4 °C (Figure 7). SdgPDH appears due to the loss of a peptide of ~20 kDa from the C-terminus of the protein even in the absence of any proteolytic activity.

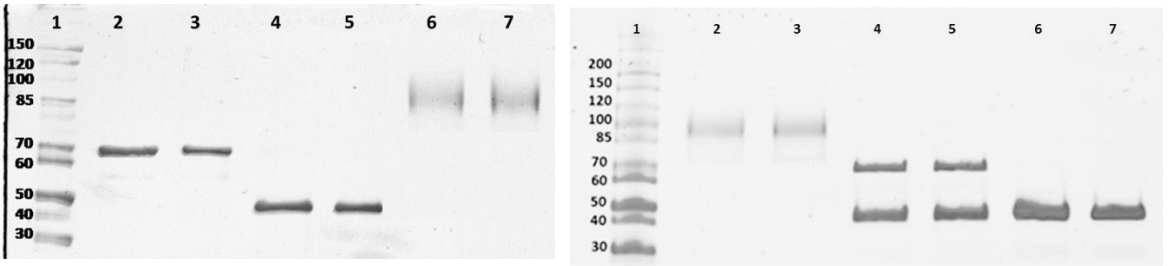

Figure 7. Characterization of enzyme decomposition in time by using 10% acrylamide SDS-PAGE with silver staining: (A) *lane 1* – molecular weight standard; *lanes 2,3* – dgPDH; *lanes 4,5* – sdgPDH; *lanes 6,7* – gPDH; (B) *lane 1* – molecular weight standard; *lanes 2,3* – gPDH; *lanes 4,5* – sdgPDH (after 2 weeks); *lanes 6,7* – sdgPDH (after 3 month) The enzyme solutions were kept at 4 ^{0}C.

3.5.2. Spectrophotometric activity assay

Volumetric activity of sdgPDH was measured within the period of three months with ferrocenium ion as electron acceptor and glucose as substrate. From

Figure **8** it can be seen that the activity of the dgPDH was increasing gradually reaching of a plateau after about two months, while for gPDH there no activity changes were observed.

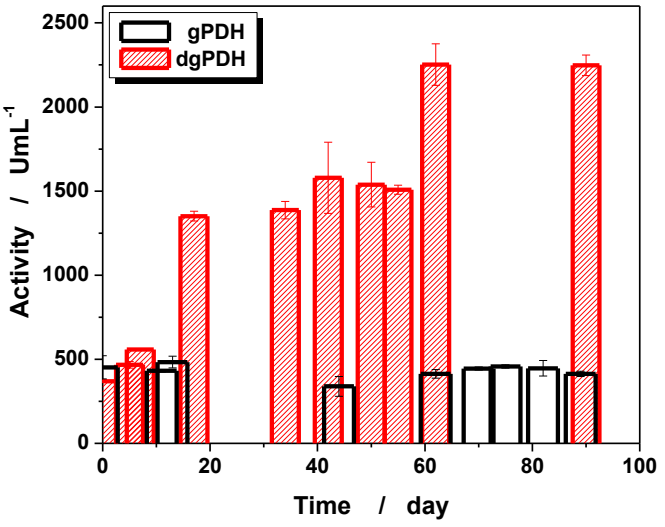

Figure 8. The change in time of the enzymatic activity of gPDH and dgPDH. Volumetric activity was measured using glucose as a substrate and ferrocenium ion (Fc^{+}) as electron acceptor (*see Experimental part*)

3.5.3. Electrocatalytic oxidation of glucose at gPDH, dgPDH and sdgPDH modified electrodes

SdgPDH enzyme loses part of its C-terminal fragment which might make shorter the distance between the active center and the mediator, thus facilitating the transfer of the electrons. To investigate these matters the electrochemical behavior of sdgPDH was measured using CV *(results in the thesis)* and amperometry in a FI system when the enzyme was co-immobilized with an Os-RP in presence of PEGDGE on the surface of a graphite electrode, as described in (Killyeni *et al.* 2012). Catalytic properties of sdgPDH were compared in terms of current output to those obtained under similar experimental conditions for gPDH and dgPDH.

The corresponding calibration curves for glucose are showed in Figure 9. The kinetic parameters corresponding to the investigated bioelectrodes were estimated by fitting the calibration curves for glucose to the Michaelis-Menten equation.

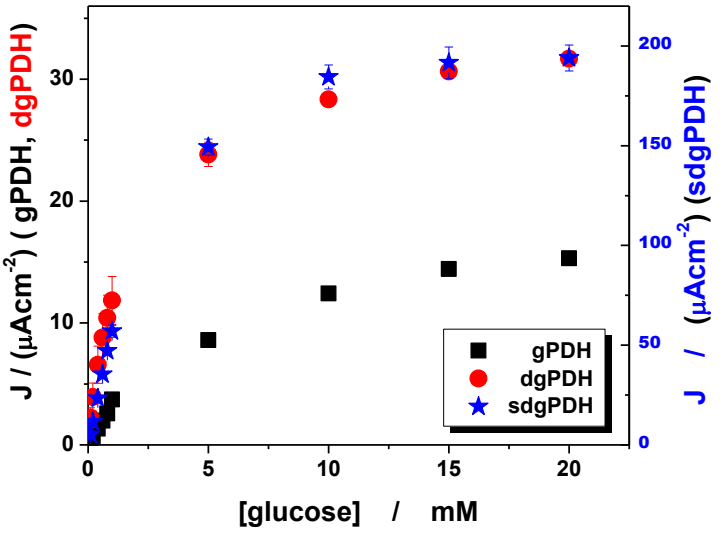

Figure 9. Calibration curves of G/gPDH-(Os-RPII), G/dgPDH-(Os-RPII) and G/sdgPDH-(Os-RPII) bioelectrodes using glucose as substrate.
Experimental conditions: applied potential, +200 mV vs. Ag|AgCl, 0.1M KCl; supporting electrolyte, 50 mM PB containing 137 mM NaCl (pH 7.4); flow rate, 0.45 mL/min.

A strong increase in the maximum catalytic current density [j_{max} = (230.8 ± 4.9) µAcm^{-2}] can be observed in case of G/sdgPDH-(Os-RPII) modified electrode compared with G/gPDH-(Os-RPII) [j_{max} = (16.3 ± 0.7) µAcm^{-2}] and G/dgPDH-(Os-RPII) [j_{max} = (33.9 ± 0.4) µAcm^{-2}] pare. The estimated apparent Michaelis-Menten constant for both dgPDH [K_M^{app} = (1.8 ± 0.1) mM] and sdgPDH [K_M^{app} = (3.0 ± 0.2) mM] compared to gPDH [K_M^{app} = (5.5 ± 0.5) mM] indicate a:

- higher enzyme-substrate affinity in case of sdgPDH and dgPDH modified bioelectrodes;
- higher permeability to glucose of the deglycosylated enzyme matrix, meaning that the substrate diffusion into the active site of deglycosylated and fragmented forms of PDH is easier.

Both increase in current output for sdgPDH and decrease in K_M^{app} support the idea that spontaneous cleavage of C-terminal fragment plays an important role in catalytic performance of the remaining part of the decomposed enzyme.

4. KINETIC STUDY OF S-ACETYL-CALIX[8]ARENE ADSORPTION AND REORGANIZATION ON POLYCRYSTALLINE GOLD SURFACE

The present study (Killyeni *et al.* 2013) was done aiming at obtaining a modified electrode incorporating a calixarene derivative. Due to the well-known recognition properties of the calixarene molecule, it was presumed that the resulting calixarene-modified electrode will exhibit interesting recognition abilities for a particular chemical species, depending on the nature of the immobilized calixarene.

For this purpose, exploiting the strong interaction between the S atoms and the Au surface, a film of thioacetylated calix[8]arene derivative (S-Calix) was formed, by simple adsorption, on the surface of polycrystalline Au. By using EIS measurements the kinetics of the S-Calix adsorption on Au, as well as the kinetics of an unexpected reorganization process involving the SAM built up on polycrystalline Au were monitored. Taking into account the peculiar S-Calix structure an explanation for this reorganization process was attempted.

Au/S-Calix modified electrode was prepared by immersing a clean Au wire in an appropriate solution of a new thioacetylated calix[8]arene derivative.

4.1. CV measurements

Qualitatively, the adsorption of S-Calix on Au was put in evidence by comparing the voltammetric response of HCF(III/II) probe recorded at bare and Au/S-Calix electrodes (Figure 10). At bare Au electrode, the voltammogram exhibits a well-defined pair of peaks, characteristic for a dissolved reversible redox couple. In contrast, after S-Calix adsorption, both peak currents decreased while the peak separation increased, proving that the adsorbed molecules of S-Calix partially blocked the access of the redox probe to the Au surface. Additionally, it is worth to mention that in the investigated potential domain no additional peaks due to the presence of S-Calix were observed.

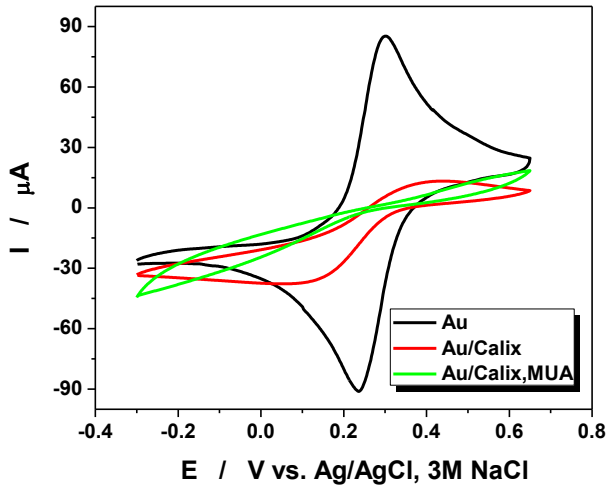

Figure 10. Voltammetric response of 5 mM HCF(II)/(III) recorded at bare Au, Au/S-Calix and Au/S-Calix,MUA electrodes.
E*xperimental conditions: scan rate, 50 mV/s; starting potential, −0.3 V vs. Ag|AgCl, 3M NaCl; supporting electrolyte, 1 M KCl.*

The CV response of Au/S-Calix modified electrode shows the features corresponding to the spherical diffusion, suggesting that the surface of Au electrode was not entirely blocked by S-Calix adsorption. This supposition was checked by recording the CV response of HCF(III/II) at Au/S-Calix,MUA modified electrode, when, due to the higher ability of MUA to form a compact monolayer on the Au surface than that corresponding to S-Calix, the electrode response was almost completely blocked.

4.2. EIS measurements

4.2.1. S-Calix adsorption

To investigate the kinetics of S-Calix adsorption on Au, impedance spectra were successively recorded at intervals of 87 s, during the adsorption process (4 h). 23 values of frequency (from100 Hz up to 23 kHz) were used for each impedance spectra.
An AC signal of 10 mV amplitude was superposed on the dc potential, which was chosen identical to the open circuit potential (OCP).

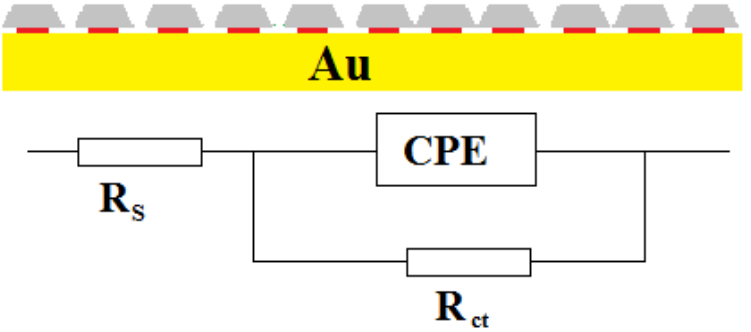

Figure 11. Equivalent circuits used for modeling the EIS recorded, to monitor the S-Calix adsorption on Au electrode. The elements of the equivalent circuits are: R_s is the resistance of the electrolyte solution; R_{ct} is the charge transfer resistance; *CPE* is the constant phase element.

The evolution in time of the calculated values corresponding to the elements from the equivalent circuit (Figure 11), together with their standard errors (95% confidence), Chi^2 values and the number of the experimental points are summarized in Table 2.

The adsorption of S-Calix on Au electrode was described with two kinetic models (Subramanian *et al.* 2000):

1. **Diffusion controlled adsorption**, described with the following relation:

$$\theta(t) = k_d C t^{1/2} \quad (1)$$

where: θ(t) is the electrode coverage; C is the S-Calix concentration; t is the time; $k_d=(4D/\Gamma^2\pi)^{1/2}$ is the diffusion rate constant; D is the S-Calix diffusion coefficient; Γ is the surface coverage at saturation. This model suitable for the initial part of the adsorption process (t < 20 min) (Figure 12);

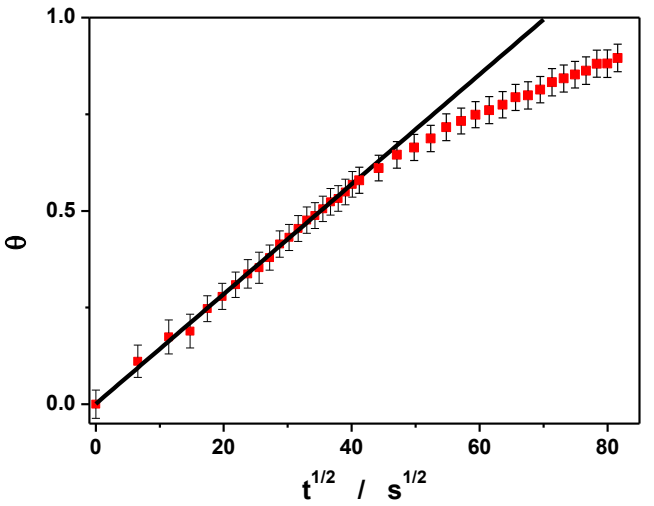

Figure 12. The variation of the surface coverage for S-Calix adsorption on Au electrode with $t^{1/2}$.

Experimental conditions: applied dc potential (OCP), 0.33 V vs. Ag|AgCl, 3 M NaCl; frequency range, from 100 Hz to 23 kHz (23 individual values); ac amplitude, 10 mV; working solution, 1.16 mg/L S-Calix in $CHCl_3/C_2H_5OH$ 1:1 (v/v) containing 0.05 M $LiClO_4$ as supporting electrolyte. Error bars stand for the half width of the 95% confidence interval

2. **Langmuir model**, described with the following relation:

$$\theta(t) = 1 - \exp(-k_m t) \qquad (2)$$

where: θ(t) is the electrode coverage; t is the time; k_m is the apparent first order rate constant for the adsorption process. Fitting well the final part of the adsorption process (t > 20 min) (Figure 13).

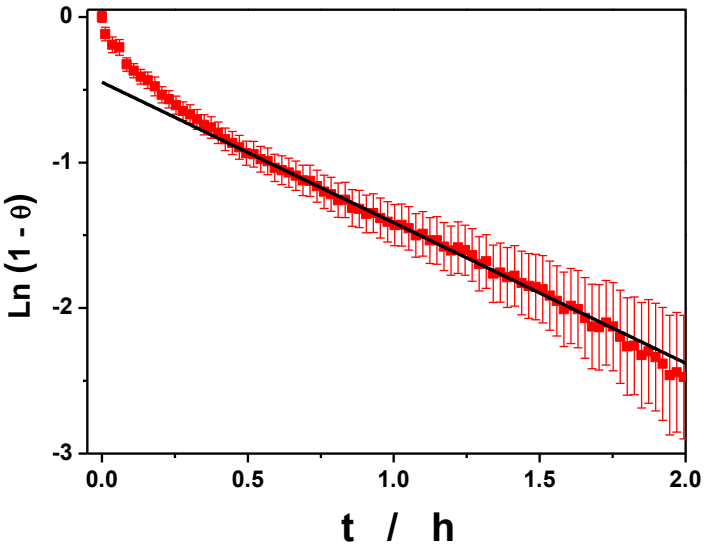

Figure 13. The variation of ln(1 − θ) with time.

Experimental conditions: see Figure 12.

Table 2. Time evolution of R_s, R_{ct}, Q and α parameters (equivalent circuit from Figure 11) during S-Calix adsorption on Au electrode.

Time (s)	**R_s (Ω cm^2)**	**R_{ct} (kΩ cm^2)**	**Q (MΩ^{-1}cm^{-2}s$^{\alpha}$)**	**a**	**Chi^2 / N (Ω^2 cm^4)**
0	75.30 ± 0.33	0.97 ± 0.16	6.127 ± 0.075	0.669 ± 0.034	0.81 / 23
304	75.21 ± 0.35	0.98 ± 0.14	5.551 ± 0.067	0.644 ± 0.034	0.89 / 23
652	74.82 ± 0.41	1.13 ± 0.19	5.344 ± 0.081	0.598 ± 0.042	1.19 / 23
1000	75.14 ± 0.38	1.09 ± 0.16	5.143 ± 0.064	0.635 ± 0.036	1.06 / 23
2044	75.32 ± 0.41	1.23 ± 0.19	4.828 ± 0.062	0.616 ± 0.037	1.18 / 23
3001	75.25 ± 0.42	1.30 ± 0.20	4.649 ± 0.060	0.607 ± 0.038	1.27 / 23
5002	74.48 ± 0.44	1.32 ± 0.19	4.406 ± 0.055	0.604 ± 0.038	1.35 / 23
8047	73.20 ± 0.48	1.44 ± 0.19	4.099 ± 0.053	0.585 ± 0.041	1.58 / 23
14050	73.56 ± 0.47	1.46 ± 0.21	4.062 ± 0.069	0.590 ± 0.039	1.63 / 23

4.2.2. Reorganization process of S-Calix monolayer

CV measurements pointed out that the S-Calix layer, self-assembled on the Au surface, undergoes a slow evolution in time, probably due to its reorganization and resulting in an increase of the surface coverage of the Au/S-Calix modified electrode. This reorganization process was explored by carrying out long time and repetitive EIS measurements at Au/S-Calix modified electrodes, at applied potentials which involve low overpotential values. The obtained Nyquist plots, relying on 57 values of frequency (from 0.01 Hz to 100 kHz), exhibit the typical features of a process con-trolled by activation and diffusion.

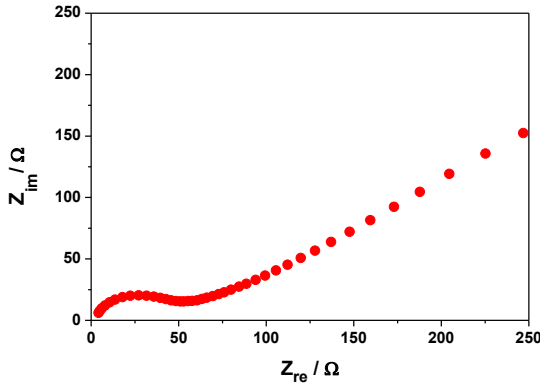

Figure 14. EIS recorded at bare Au electrode.
Experimental conditions: applied dc potential, +0.24 V vs. Ag|AgCl, 3M NaCl; frequency range, from 10 mHz to 100 kHz (57 individual values); ac amplitude, 10 mV; supporting electrolyte, 1 M KCl.

As can be seen from

Figure 15, irrespective of recording time, all spectra consist of a depressed semi-circle (generated by the charge transfer process and located in the domain of high frequencies) coupled with a Warburg transmission line (corresponding to the diffusion of the redox couple and situated in the domain of low frequencies). This behavior is similar to that noticed for bare Au electrode (Figure 14), with the exception that a much faster charge transfer was observed for the naked electrode. In time, the charge transfer, represented with the semi-circles in Nyquist plots, showed a monotone decrease, suggesting an increase of the electrode blocked surface. Probably this behavior is a consequence of the increase of the electrode coverage, induced by a rearrangement of the S-Calix immobilized in the self-assembled layer.

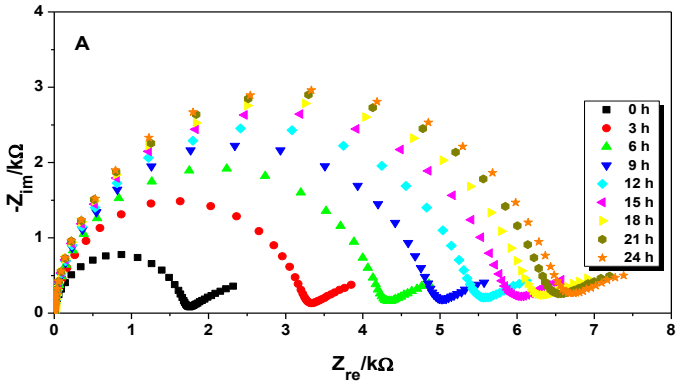

Figure 15. EIS recorded successively at Au/S-Calix modified electrode in pH 7.
Experimental conditions: see Figure 14.

Taking into account that, even after large time intervals (t > 20 h), on the recorded impedance spectra can be still observed the charge transfer semi-circles, it can be stated that the S-Calix layer, formed and reorganized on the electrode surface, does not completely block the electron transfer ability of the Au surface. This hypothesis was

confirmed, qualitatively, by the significant decrease of the semi-circle diameter noticed on the impedance spectra recorded at Au/S-Calix,MUA modified electrode, which corroborates well with the CV response recorded at the same electrode.

An attempt to rationalize the impedance spectra recorded during the reorganization of S-Calix layer formed on the Au surface was carried out by their modeling using the equivalent circuit presented in Figure 16. This equivalent circuit starts from the model proposed by Finklea (Finklea *et al.* 1993; Rueda *et al.* 2011) for active pinholes surrounded by inactive areas behaving as an array of ultra-microelectrodes, which was adapted for "inactive" areas of a certain activity. This basic idea seems reasonable taking into consideration the peculiar conformation of S-Calix molecules, which are expected to build less compact adsorbed layer in comparison with the thioalkanes.

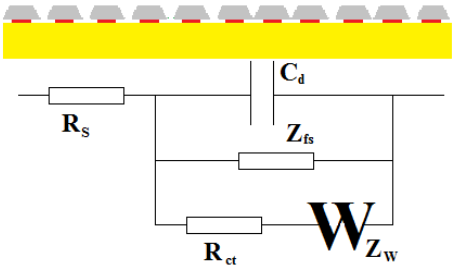

Figure 16. Equivalent circuits used for modeling the EIS recorded during the SAM reorganization on Au/S-Calix modified electrode. The elements of the equivalent circuits are: R_s is the resistance of the electrolyte solution; R_{ct} is the charge transfer resistance; C_d is the double layer capacitance and Z_w is the Warburg diffusion impedance.

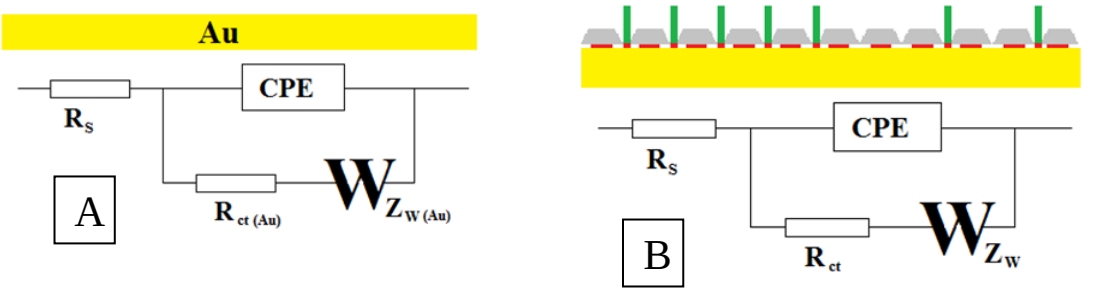

Figure 17. Equivalent circuits used for modeling the EIS recorded: (A) at a bare Au electrode and (B) Au/S-Calix,MUA electrode. The elements of the equivalent circuits are: R_s is the resistance of the electrolyte solution; R_{ct} is the charge transfer resistance; CPE is the constant phase element and Z_w is the Warburg diffusion impedance.

The supplementary data, necessary to model the equivalent circuit, were obtained by modeling the impedance spectra recorded at bare Au using the equivalent circuit from Figure 17 (A) and Au/S-Calix,MUA electrodes from Figure 17 (B). In all cases, a complex non-linear least squares fitting procedure, based on Levenberg–Marquardt algorithm implemented in Origin 8.5 (Origin Lab, USA), was used to estimate the free coverage for the Au/S-Calix modified electrode from the corresponding experimental impedance spectra.

The data resulted from the modeling of impedance spectra recorded at Au and Au/S-Calix,MUA electrodes (Table 3) combined with those provided by the impedance spectra modeling of Au/S-Calix electrode, allowed the calculation of the coverage for Au/S-Calix electrode for different time intervals (Table 4).

Table 3. Calculated values of the parameters used for modeling the EIS recorded at bare Au and Au/S-Calix,MUA electrodes (equivalent circuit from Figure 17Error! Reference source not found.**)**

Electrode	pH	R_s (Ω cm^2)	R_{ct} (Ω cm^2)	Q ($M\Omega^{-1}$ cm^{-2} s$^{\alpha}$)	α	σ (Ω s$^{-1/2}$ cm^2)	Chi^2 / N (Ω^2 cm^4)
Au	5	0.93 ± 0.74	5.23 ± 1.29	615 ± 124	0.55 ± 0.10	22.8 ± 0.2	0.00001 / 57
	7	0.45 ± 0.38	10.29 ± 0.80	161 ± 44	0.75 ± 0.03	28.2 ± 0.6	0.00006 / 57
Au/S-Calix,MUA	5	0.87 ± 1.11	655.7 ± 1.2	6.12 ± 0.07	0.940 ± 0.002	30.6 ± 0.4	2.66 / 57
	7	1.37 ± 1.58	2440.9 ± 3.8	6.61 ± 0.05	0.943 ± 0.002	28.7 ± 1.2	33.32 / 57

Table 4. Time evolution of the parameters of the equivalent circuit presented in Figure 16 used to monitor the reorganization of S-Calix layer self-assembled on Au electrode.

Electrode	pH	Time (h)	R_s (Ω cm^2)	C_d (μF cm^{-2})	1-θ (%)	q (s^{-1})	Chi^2 / N (Ω^2 cm^4)
Au/S-Calix	5	0	0.86 ± 1.53	2.82 ± 0.62	3.96 ± 0.19	245 ± 55	61.3 / 57
		6	0.50 ± 2.67	2.89 ± 0.26	1.42 ± 0.03	236 ± 34	110.5 / 57
		12	1.06 ± 3.80	2.76 ± 0.27	0.95 ± 0.03	222 ± 33	161.4 / 57
		18	0.89 ± 7.02	2.67 ± 0.47	0.77 ± 0.04	189 ± 28	249.7 / 57
	7	0	3.17 ± 0.76	5.39 ± 0.03	4.59 ± 0.02	334 ± 13	0.9 / 57
		6	4.07 ± 1.39	4.92 ± 0.03	1.53 ± 0.01	221 ± 12	7.2 / 57
		12	4.22 ± 2.56	4.64 ± 0.05	1.09 ± 0.01	171 ± 13	29.3 / 57
		18	4.12 ± 3.63	4.46 ± 0.06	0.90 ± 0.01	149 ± 14	62.1 / 57

The data summarized in Table 4 clearly point out that the S-Calix layer undergoes a slow reorganization process involving the already immobilized S-Calix molecules and inducing a significant decrease of the electrode free surface (see the sixth column of Table 4). The variation of the free coverage in time under the reorganization process of the SAM layer is presented in Figure 18. It is worth mentioning that the total decrease of the free coverage agrees to the current decrease observed on the CV recorded at Au/S-Calix electrode (see Figure 10).

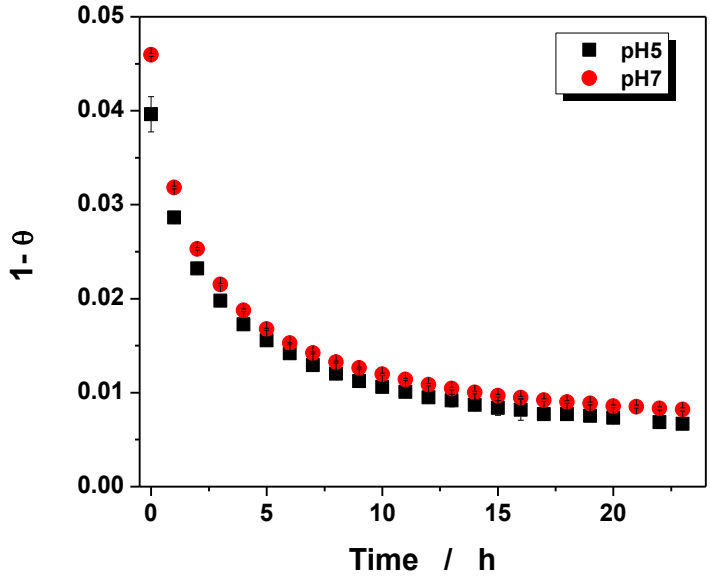

Figure 18. Time evolution of the free surface ratio (1− θ) for Au/S-Calix modified electrode; at pH 5 and pH 7. Error bars stand for the half width of the 95% confidence interval.

Essentially, the reorganization process consists in the increase of the S – Au bonds for the already immobilized S-Calix molecules *via* adequate conformational conversions of the S-Calix molecules. This process is driven by the remarkable high affinity between S and Au atoms, which favors the binding of all S atoms from the S-Calix molecule. On the other, the reorganization process is facilitated by the well-known flexibility of the calix[8]arene skeleton, allowing a multitude of conformations, even enhanced by the presence of small-size substituents, such as – S – CO – CH_3 (on the upper rim) and – O – CH_3 (on the lower rim) (Neri *et al.* 2002). Investigations on the applications of the Au/S-Calix modified surfaces, as materials exhibiting properties of ion/molecule recognition or useful for the selective transport of biological active chemical species, are in progress.

5. GENERAL CONCLUSIONS

I. The effect of deglycosylation of *Am*PDH overexpressed in *Pichia pastoris* was studied using PDHs modified electrodes. The stability of dgPDH enzyme in solution was followed using SDS-PAGE and UV/Vis measurements. Biocatalytic activity of PDHs modified electrodes was evaluated using CV and FI measurements.

- From SDS-PAGE measurements it can be seen that, as a consequence of its expression in *Pichia pastoris* host organism, gPDH is highly glycosylated and by partially removing of the glycan shell its mass decreases from 95-100 kDa to ~65 kDa (the deference being the glycan moiety from the peptide chain).
- CV measurements allowed the estimation of the catalytic efficiency for the *Am*PDHs modified electrodes, indicating that the G/dgPDH-(Os-RPII) bioelectrode exhibits a slightly higher value than observed for the G/gPDH(Os-RPII) bioelectrode.
- For the same enzyme loading (expressed in U/cm^2), the G/dgPDH-(Os-RPII) bioelectrode exhibits a higher amperometric response compared with the G/gPDH-(Os-RPII) bioelectrode. At the same time, *Am*PDH deglycosylation resulted in a lower value of the apparent Michaelis-Menten constant, compared with that estimated for the initial enzyme.
- The *Am*PDH deglycosylation induces significant changes in the order of the substrate selectivity:

gPDH: Glucose > Fucose > Galactose > Cellobiose > Xylose > Sucrose > Maltose > Lactose > 2-Deoxy-*D*-glucose > Mannose

dgPDH: Fucose > Glucose > Xylose > Sucrose > Galactose > Cellobiose > Maltose > 2-Deoxy-*D*-glucose > Lactose > Mannose

- Deglycosylated PDH based bioelectrode shows a slightly better short time stability than the glycosylated PDH based bioelectrode.
- It was discovered that after two months storing at 4 °C, dgPDH loses a peptide fragment from C-terminal. The resulting enzyme (sdgPDH) has a MW of ~46 kDa and possesses higher enzymatic activity compared to the glycosylated and deglycosylated ones.

II. The second part of the present work was dedicated to the investigation of the S-Calix adsorption and the reorganization processes of the resulted SAM on polycrystalline Au surface, by using CV, Raman spectroscopy, QCMB and EIS measurements.

- CV measurements performed in presence of HCF(III/II) redox couple, evidenced a time evolution of the permeability of S-Calix layer formed by simple adsorption on Au surface. The voltammetric response observed at Au/S-Calix modified electrodes suggests a reorganization process occurring within the self-assembled layer of S-Calix, and resulting in the increase of the blocked surface on the aged Au/S-Calix electrodes.
- EIS measurements were used to describe the S-Calix adsorption process. Thus, at the beginning the adsorption process shows the characteristics of a pure diffusion controlled process, but furthermore it obeys the Langmuir model;
- At the end of adsorption process ($\theta > 0.9$) a slow reorganization process occurs, consisting in the increase of the number of S – Au bonds for the already adsorbed S-Calix

molecules. This reorganization process is driven by the high affinity existing between the S and Au atoms and is facilitated by the remarkable flexibility of the calix[8]arene skeleton. At steady state the S-Calix molecules are organized in a monolayer on the Au polycrystalline surface, each molecule being attached through 3–4 S atoms

- It can be stated that the self-assembling of Au/S-Calix structures offers a simple, rapid, and efficient way for a versatile design of smart materials, exhibiting interesting properties for ionic or molecular recognition.

6. SCIENTIFIC ACTIVITY

6.1. Papers

I. **Maria** E. Yakovleva, **Aniko Killyeni**, Roberto Ortiz, Christopher Schulz, Domhnall MacAodha, Peter Ó. Conghaile, Dónal Leech, Ionel Catalin Popescu, Christoph Gonaus, Clemens K. Peterbauer, Lo Gorton, (**2012**) *Recombinant pyranose dehydrogenase — A versatile enzyme possessing both mediated and direct electron transfer*. Electrochemistry Communications 24, 120–122

II. **Aniko Killyeni,** Maria E. Yakovleva, Clemens K. Peterbauer, Dónal Leech, Lo Gorton, Ionel Catalin Popescu, (**2012**) *Effect of enzyme deglycosylation on the amperometric detection of glucose at PDH-modified electrode,* Studia Universitatis Babes-Bolyai, Seria Chemia 4, 87-99

III. **Aniko Killyeni**, Adrian Nicoara, Vali Canpean, Attila Kun, Simion Astilean, Ionel Catalin Popescu, (**2013**) *S-acetyl-calix[8]arene adsorption on polycrystalline Au surface: A kinetic study*, Electrochimica Acta 102, 225–232

IV. **Anikó Killyéni**, Maria E. Yakovleva, Domhnall MacAodha, Peter Ó Conghaile, Christoph Gonaus, Dónal Leech, Ionel Catalin Popescu, Clemens K. Peterbauer, Lo Gorton, **(2013)** *Effect of deglycosylation on the mediated electrocatalytic activity of recombinantly expressed Agaricus meleagris pyranose dehydrogenase wired by ososmium- redox polymer,* Electrochimica Acta (subbmited)

V. Maria Yakovleva, **Anikó Killyéni**, Oliver Seubert, Peter Ó Conghaile, Domhnall MacAodha, Dónal Leech, Christoph Gonaus, Ionel Catalin Popescu, Clemens K. Peterbauer, Sven Kjellström, Lo Gorton, (2013) Further insights into the catalytical properties of deglycosylated pyranose dehydrogenase from Agaricus meleagris recombinantly expressed in Pichia pastoris, Electrochimica Acta (submitted)

6.2. Conferences participation

I. **Anikó Killyéni**, Adrian Nicoara, Graziella Liana Turdean, Ionel Catalin Popescu, (**2011**) *Electrochemical investigation of self-assembled calixarenes on gold.* 17th International Conference of Chemistry, Cluj-Napoca, Romania, 4-6 November (poster presentation)

II. **Aniko Killyeni**, Vali Canpean, Adrian Nicoara, Graziella Liana Turdean, Ionel Catalin Popescu, Simion Astilean, (**2011**) *Electrochemical investigation of self-assembled S-acetyl-calix[8]arene on gold for molecular recognition.* Advance Spectroscopies on Biomedical Nanostructured Systems (BioNanoSpec) 7 September (oral presentation)

III. **Aniko Killyeni,** Maria E. Yakovleva, Lo Gorton, Ionel Catalin Popescu, (**2012**) *Effect of PDH deglycosylation on the glucose amperometric detection*. 18th International Conference of Chemistry, Cluj-Napoca, Romania, 23-25 November (oral presentation)

IV. **Anikó Killyéni**, Maria Yakovleva, Lo Gorton, Ionel Catalin Popescu, (**2013**) *Effect of Deglycosylation on the Selectivity of Agaricus meleagris Pyranose Dehydrogenase Modified Electrodes*. 12th Topical Meeting of the International Society of Electrochemistry/XXII International Symposium on Bioelectrochemistry and Bioenergetics of the Bioelectrochemical Society, 17-21 March (poster presentation)

V. Maria Yakovleva, **Anikó Killyéni**, Clemens K. Peterbauer, Ionel Catalin Popescu, Lo Gorton, (**2013**) *Further insights into catalytical properties of deglycosylated pyranose dehydrogenase from Agaricus meleagris recombinantly expressed in Pichia pastoris.* 12th Topical Meeting of the International Society of Electrochemistry/XXII International Symposium on Bioelectrochemistry and Bioenergetics of the Bioelectrochemical Society, 17-21 March (oral presentation)

VI. **Anikó Killyéni**, Maria Yakovleva, Lo Gorton, Ionel Catalin Popescu, (**2013**) *Improved biosensors by deglycosylation of pyranose dehydrogenase isolated from Agaricus meleagris.* 4th Regional Symposium on Electrochemistry South East Europe, 26 - 30 May (poster presentation)

VII. Adrian Nicoara, **Anikó Killyéni**, Ionel Catalin Popescu (**2013**) *Formation and reorganization kinetics of self-assembled calixarene on gold* 4th Regional Symposium on Electrochemistry South East Europe, 26 - 30 May (poster presentation)

7. SELECTIVE REFERENCES

Bartsch, H., Arndt, C., Koristka, S., Cartellieri, M., Bachmann, M., **2012.** *Silver staining techniques of polyacrylamide gels.* . In: Kurien, B.T., Scofield, R.H. (Eds.), Protein Electrophoresis, pp. 481-486. Humana Press.

Becker, A., Tobias, H., Porat, Z., Mandler, D., (**2008);** *Detection of uranium(VI) in aqueous solution by a calix[6]arene modified electrode*, Journal of Electroanalytical Chemistry 621(2), 214-221.

Bian, Y., Li, C., Li, H., (**2010);** *para-Sulfonatocalix[6]arene-modified silver nanoparticles electrodeposited on glassy carbon electrode: Preparation and electrochemical sensing of methyl parathion*, Talanta 81(3), 1028-1033.

Buck, M., **2009.** *Structure, Electrochemistry and Applications of Self-Assembled Monolayers of Thiols*. Chemically Modified Electrodes, pp. 197-255. Wiley-VCH Verlag GmbH & Co. KGaA.

Chen, D., Shen, M., Cao, Y., Bo, B., Chen, Z., Shu, Y., Li, G., (**2013);** *Electrochemical identification of hepatocellular carcinoma based on the assay of human cervical cancer oncoprotein-1 in serum*, Electrochemistry Communications 27(0), 38-41.

Chen, H., Gal, Y.-S., Kim, S.-H., Choi, H.-J., Oh, M.-C., Lee, J., Koh, K., (**2008);** *Potassium ion sensing using a self-assembled calix[4]crown monolayer by surface plasmon resonance*, Sensors and Actuators B: Chemical 133(2), 577-581.

Chen, H., Huang, J., Lee, J., Hwang, S., Koh, K., (**2010a);** *Surface plasmon resonance spectroscopic characterization of antibody orientation and activity on the calixarene monolayer*, Sensors and Actuators B: Chemical 147(2), 548-553.

Chen, S., Webster, R.D., Talotta, C., Troisi, F., Gaeta, C., Neri, P., (**2010b);** *Electrochemistry and ion-sensing properties of calix[4]arene derivatives*, Electrochim. Acta 55(23), 7036-7043.

Chung, T.D., Park, J., Kim, J., Lim, H., Choi, M.-J., Kim, J.R., Chang, S.-K., Kim, H., (**2001);** *Self-Assembled Monolayer of a Redox-Active Calix[4]arene: Voltammetric Recognition of the Ba2+ Ion in Aqueous Media*, Analytical Chemistry 73(16), 3975-3980.

Courjean , O., Flexer , V., Prévoteau , A., Suraniti , E., Mano, N., (**2010);** *Effect of Degree of Glycosylation on Charge of Glucose Oxidase and Redox Hydrogel Catalytic Efficiency*, ChemPhysChem 11(13), 2795-2797.

Ferapontova, E.E., Grigorenko, V.G., Egorov, A.M., Borchers, T., Ruzgas, T., Gorton, L., (**2001);** *Direct electron transfer in the system gold electrode-recombinant horseradish peroxidases*, Journal of Electroanalytical Chemistry 509(1), 19-26.

Ferapontova, E.E., Shleev, S., Ruzgas, T., Stoica, L., Christenson, A., Tkac, J., Yaropolov, A.I., Gorton, L., **2005.** *Direct Electrochemistry of Proteins and Enzymes*. In: Emil Paleček, F.S., Wang, J. (Eds.), Perspectives in Bioanalysis, pp. 517-598. Elsevier.

Finklea, H.O., Snider, D.A., Fedyk, J., Sabatani, E., Gafni, Y., Rubinstein, I., (**1993);** *Characterization of octadecanethiol-coated gold electrodes as microarray electrodes by cyclic voltammetry and ac impedance spectroscopy*, Langmuir 9(12), 3660-3667.

Fraser, D.M., Zakeeruddin, S.M., Grätzel, M., (**1992);** *Mediation of glycoslated and partially-deglycosylated glucose oxidase of Aspergillus niger by a ferrocene-derivatised detergent*, Biochimica et Biophysica Acta (BBA) - Bioenergetics 1099(1), 91-101.

Frew, J.E., Hill, H.A.O., Thomas, J.D.R., (**1987);** *Electron-Transfer Biosensors [and Discussion]*, Phil. Trans. R. Soc. Lond. B 316, 95-106.

Gutsche, D., (**2008**); *Calixarenes An Introduction*, 2nd Ed ed. RSC Publishing, Cambridge.

Hassen, W.M., Martelet, C., Davis, F., Higson, S.P.J., Abdelghani, A., Helali, S., Jaffrezic-Renault, N., (**2007);** *Calix[4]arene based molecules for amino-acid detection*, Sensors and Actuators B: Chemical 124(1), 38-45.

Huang, L., Reekmans, G., Saerens, D., Friedt, J.-M., Frederix, F., Francis, L., Muyldermans, S., Campitelli, A., Hoof, C.V., (**2005);** *Prostate-specific antigen immunosensing based on mixed self-assembled monolayers, camel antibodies and colloidal gold enhanced sandwich assays*, Biosensors and Bioelectronics 21(3), 483-490.

Killyeni, A., Nicoara, A., Canpean, V., Kun, A., Astilean, S., Popescu, I.C., (**2013);** *S-acetyl-calix[8]arene adsorption on polycrystalline Au surface: A kinetic study*, Electrochim. Acta 102(0), 225-232.

Killyéni, A., Yakovleva, M.E., MacAodha, D., Conghaile, P.Ó., Gonaus, C., Leech, D., Popescu, I.C., Peterbauer, C.K., Gorton, L., (**2013);** *Effect of deglycosylation on the mediated electrocatalytic activity of recombinantly expressed Agaricus meleagris pyranose dehydrogenase wired by ososmium- redox polymer*, Electrochim. Acta subbmited.

Killyeni, A., Yakovleva, M.E., Peterbauer, C.K., Leech, D., Gorton, L., Popescu, I.C., (**2012);** *Effect of enzyme deglycosylation on the amperometric detection of glucose at PDH-modified electrode*, Studia Universitatis Babes-Bolyai, Seria Chemia 4.

Lindgren, A., Tanaka, M., Ruzgas, T., Gorton, L., Gazaryan, I., Ishimori, K., Morishima, I., (**1999);** *Direct electron transfer catalysed by recombinant forms of horseradish peroxidase: insight into the mechanism*, Electrochemistry Communications 1(5), 171-175.

Lucke, A.J., Stirling, C.J.M., **2000.** *Calixarenes in Thin Film Supramolecular Materials*. In: L. Mandorlini, Ungaro, R. (Eds.), Calixarenes in Action, pp. 172-202. Imperial College Press, London.

Mechref, Y., Novotny, M.V., (**2002);** *Structural Investigations of Glycoconjugates at High Sensitivity*, Chemical Reviews 102(2), 321-370.

Neri, P., Consoli, G.L., Cunsolo, F., Geraci, C., Piattelli, M., **2002.** *Chemistry of Larger Calix[n]aremes (n=7, 8, 9)*. In: Asfari, Z., Böhmer, V., Harrowfield, J., Vicens, J., Saadioui, M. (Eds.), Calixarenes 2001, pp. 89-109. Springer Netherlands.

Ortiz, R., Matsumura, H., Tasca, F., Zahma, K., Samejima, M., Igarashi, K., Ludwig, R., Gorton, L., (**2012);** *Effect of Deglycosylation of Cellobiose Dehydrogenases on the Enhancement of Direct Electron Transfer with Electrodes*, Analytical Chemistry 84(23), 10315-10323.

Patel, G., Menon, S., (**2009);** *Recognition of lysine, arginine and histidine by novel p-sulfonatocalix[4]arene thiol functionalized gold nanoparticles in aqueous solution*, Chemical Communications(24), 3563-3565.

Peterbauer, C.K., Volc, J., (**2010);** *Pyranose dehydrogenases: biochemical features and perspectives of technological applications*, Appl. Microbiol. Biotechnol. 85(4), 837-848.

Presnova, G., Grigorenko, V., Egorov, A., Ruzgas, T., Lindgren, A., Gorton, L., Borchers, T., (**2000);** *Direct heterogeneous electron transfer of recombinant horseradish peroxidases on gold*, Faraday Discussions 116, 281-289.

Prévoteau, A., Courjean, O., Mano, N., (**2010);** *Deglycosylation of glucose oxidase to improve biosensors and biofuel cells*, Electrochemistry Communications 12(2), 213-215.

Rueda, M., Prieto, F., (**2011);** *Application of electrochemical impedance spectroscopy tothe study of surface processes*, Collection of Czechoslovak Chemical Communications 76, 1825.

Sakly, H., Mlika, R., Bonnamour, I., Aouni, F., Ouada, H.B., Renault, N.J., (**2007);** *Kinetic characterization of p-tert-butylcalix[4,8,12]arene functionalized gold electrode by electrochemical impedance spectroscopy*, Electrochim. Acta 52(11), 3697-3703.

Šnejdárková, M., Poturnayová, A., Rybár, P., Lhoták, P., Himl, M., Flídrová, K., Hianik, T., (**2010);** *High sensitive calixarene-based sensor for detection of dopamine by electrochemical and acoustic methods*, Bioelectrochemistry 80(1), 55-61.

Subramanian, R., Lakshminarayanan, V., (**2000);** *A study of kinetics of adsorption of alkanethiols on gold using electrochemical impedance spectroscopy*, Electrochim. Acta 45(27), 4501-4509.

Sygmund, C., Gutmann, A., Krondorfer, I., Kujawa, M., Glieder, A., Pscheidt, B., Haltrich, D., Peterbauer, C., Kittl, R., (**2012);** *Simple and efficient expression of Agaricus meleagris pyranose dehydrogenase in Pichia pastoris*, Appl. Microbiol. Biotechnol. 94(3), 695-704.

Sygmund, C., Kittl, R., Volc, J., Halada, P., Kubatova, E., Haltrich, D., Peterbauer, C.K., (**2008);** *Characterization of pyranose dehydrogenase from Agaricus meleagris and its application in the C-2 specific conversion of d-galactose*, J. Biotechnol. 133(3), 334-342.

Tasca, F., Timur, S., Ludwig, R., Haltrich, D., Volc, J., Antiochia, R., Gorton, L., (**2007);** *Amperometric Biosensors for Detection of Sugars Based on the Electrical Wiring of Different Pyranose Oxidases and Pyranose Dehydrogenases with Osmium Redox Polymer on Graphite Electrodes*, Electroanalysis 19(2-3), 294-302.

Volc, J., Sedmera, P., Halada, P., Daniel, G., Prikrylova, V., Haltrich, D., (**2002);** *C-3 oxidation of non-reducing sugars by a fungal pyranose dehydrogenase: spectral characterization*, J. Mol. Catal. B-Enzym. 17(2), 91-100.

Volc, J., Sedmera, P., Halada, P., Prikrylova, V., Daniel, G., (**1998);** *C-2 and C-3 oxidation of d-Glc, and C-2 oxidation of d-Gal by pyranose dehydrogenase from Agaricus bisporus*, Carbohydr. Res. 310(1), 151-156.

Wang, Z., Zheng, Q.Y., Chen, Y., (**2001);** *Detection of metal ions using a wavelength interrogation surface plasmon resonance sensor with calix[4]arene derivatives as sensing film*, Analytical Letters 34(15), 2609-2619.

Yakovleva, M., Killyén, A., Seubert, O., Conghaile, P., Ó , MacAodha, D., Leech, D., Gonaus, C., Popescu, I.C., Peterbauer, C.K., Kjellström, S., Gorton, L., (**2013);** *Further insights into the catalytical properties of deglycosylated pyranose dehydrogenase from Agaricus meleagris recombinantly expressed in Pichia pastoris*, manuscript.

Yakovleva, M.E., Killyéni, A., Ortiz, R., Schulz, C., MacAodha, D., Conghaile, P.Ó., Leech, D., Popescu, I.C., Gonaus, C., Peterbauer, C.K., Gorton, L., (**2012);** *Recombinant pyranose dehydrogenase—A versatile enzyme possessing both mediated and direct electron transfer*, Electrochemistry Communications 24, 120-122.

Zhang, S., Echegoyen, L., (**2003);** *Self-assembled monolayers of different conformers of p-tert-butylcalix[4]crown-6 derivatives and their metal cation recognition properties*, Tetrahedron Letters 44(51), 9079-9082.

Zhang, S., Palkar, A., Echegoyen, L., (**2006);** *Selective Anion Sensing Based on Tetra-amide Calix[6]arene Derivatives in Solution and Immobilized on Gold Surfaces via Self-Assembled Monolayers*, Langmuir 22(25), 10732-10738.

Zhang, W., Li, G., (**2004);** *Third-Generation Biosensors Based on the Direct Electron Transfer of Proteins*, Analytical Sciences 20(4), 603-609.